Clinical Neurophysiology 129 (2018) 210–221

Contents lists available at ScienceDirect

Clinical Neurophysiology

journal homepage: www.elsevier.com/locate/clinph

Abnormal cortical neural synchrony during working memory in schizophrenia

Seung Suk Kang [a,*], Angus W. MacDonald III [c,b,d], Matthew V. Chafee [d,e], Chang-Hwan Im [f], Edward M. Bernat [g], Nicholas D. Davenport [e,b], Scott R. Sponheim [e,b,c]

[a] Department of Psychiatry, University of Missouri-Kansas City, Kansas City, MO 64108, USA
[b] Department of Psychiatry, University of Minnesota, Minneapolis, MN 55455, USA
[c] Department of Psychology, University of Minnesota, Minneapolis, MN 55454, USA
[d] Department of Neuroscience, University of Minnesota, Minneapolis, MN 55455, USA
[e] Veterans Affairs Health Care System, Minneapolis, MN 55417, USA
[f] Department of Biomedical Engineering, Hanyang University, Seoul 133-791, South Korea
[g] Department of Psychology, University of Maryland, Colledge Park, MD 20742, USA

ARTICLE INFO

Article history:
Accepted 28 October 2017
Available online 6 November 2017

Keywords:
Schizophrenia
Working memory
Neural oscillation
Cortical source analysis
Magnetoencephalography (MEG)

HIGHLIGHTS

- In WM encoding, PSZ had deficient prefrontal θ ERS that predicted WM performances.
- PSZ had prefrontal and parietal β ERD reductions during prolonged WM maintenance.
- In retrieval/manipulation, PSZ had deficient γ ERS in premotor and parietal cortices.

ABSTRACT

Objective: To better understand the origins of working memory (WM) impairment in schizophrenia we investigated cortical oscillatory activity in people with schizophrenia (PSZ) while they performed a WM task requiring encoding, maintenance, and retrieval/manipulation processes of spatial information.
Methods: We examined time–frequency synchronous energy of cortical source signals that were derived from magnetoencephalography (MEG) localized to cortical regions using WM–related hemodynamic responses and individualized structural head-models.
Results: Compared to thirteen healthy controls (HC), twelve PSZ showed performance deficits regardless of WM–load or duration. During encoding, PSZ had early theta and delta event-related synchrony (ERS) deficits in prefrontal and visual cortices which worsened with greater memory load and predicted WM performance. During prolonged maintenance of material, PSZ showed deficient beta event-related desynchrony (ERD) in dorsolateral prefrontal, posterior parietal, and visual cortices. In retrieval, PSZ showed reduced delta/theta ERS in the anterior prefrontal and ventral visual cortices and diminished gamma ERS in the premotor and posterior parietal cortices.
Conclusions: Although beta/gamma cortical neural oscillatory deficits for maintenance/retrieval are evident during WM, the abnormal prefrontal theta-frequency ERS for encoding is most predictive of poor WM in schizophrenia.
Significance: Time-frequency-spatial analysis identified process- and frequency-specific neural synchrony abnormalities underlying WM deficits in schizophrenia.

1. Introduction

Working memory (WM) encompasses the encoding, maintenance, and retrieval of mental representations that guide behavior (Baddeley, 2012; Miyake and Shah, 1999). Recent experimental studies have demonstrated that people with schizophrenia (PSZ)

* Corresponding author at: 1000 E 24th St, Kansas City, MO 64108, USA.
E-mail address: kangseung@umkc.edu (S.S. Kang).

https://doi.org/10.1016/j.clinph.2017.10.024
1388-2457/

have WM storage capacity deficits which is not simply explained by instability in WM mental representation (Gold et al., 2010) or attentional deficits (Erickson et al., 2015), suggesting that problems in multiple neural processes might contribute to limited WM capacity in PSZ. Neuroimaging studies of PSZ performing WM tasks have revealed abnormalities in prefrontal and parietal cortices (Barch and Ceaser, 2012) evident during maintenance (Driesen et al., 2008) and manipulation (Cannon et al., 2005) of visual material. Additionally, electrophysiological studies have revealed that early encoding and retrieval failures in the visual system contribute to WM deficits in schizophrenia (Haenschel et al., 2007; Dias et al., 2011; Lynn et al., 2016), suggesting that such deficits are caused by abnormalities in brain regions not only involved with high level cognition but also more basic aspects of stimulus processing. Despite this evidence of abnormalities in multiple cortical areas in, little is known of the relative timing and contributions of the aberrations in neural activity underlying WM deficits in schizophrenia. We report here findings highlighting the importance of diminished early theta oscillatory activity in prefrontal cortex in accounting for WM dysfunction in schizophrenia.

Synchronization of neural oscillations reflected in the strength of activity in specific frequency ranges is thought to represent temporal coordination of neural processes that enable cognitive processes (Wang, 2010). Investigations of electric and magnetic fields of the brain provide evidence of a relationship between these neuronal oscillations and WM in humans. Increases and decreases in neural oscillatory activity (termed event-related-synchronization [ERS] and event-related-desynchronization [ERD], respectively) in several frequency bands appear to reflect sensory and cognitive functions that compose WM (see Palva and Palva, 2007; Sauseng et al., 2010; Hanslmayr et al., 2012; Roux and Uhlhaas, 2014 for review) and may point to possible origins of the deficit in PSZ (Phillips and Uhlhaas, 2015; Uhlhaas et al., 2008).

One means of determining which anomalies in the temporal dynamics of neuronal activity best explain WM deficits in schizophrenia is to improve characterization of the cortical origins of oscillations evident during the encoding, maintenance, and retrieval of information during WM. To date, the neuroanatomical sources of oscillatory abnormalities during WM in PSZ are largely unknown. Thus, it is difficult to discern how anatomical findings from imaging studies relate to the temporal dynamics of brain function. Electroencephalography (EEG) and magnetoencephalography (MEG) studies of WM in schizophrenia have demonstrated abnormal oscillatory activity in several frequency bands likely reflecting separable neural functions (Bachman et al., 2008; Basar-Eroglu et al., 2007; Haenschel et al., 2009; Ince et al., 2009; Schmiedt et al., 2005; Stephane et al., 2008); however, neuroanatomical localization of this aberrant cortical activity has yet to be achieved in schizophrenia.

To hone in on the origins of WM dysfunction in schizophrenia it is also important to isolate specific neural abnormalities to components that make up the cognitive function. PSZ have impairments in the maintenance of material in WM and demonstrate larger deficits in tasks requiring the manipulation of the material (i.e., demands on central executive functions) (Cannon et al., 2005; Kim et al., 2004; Leiderman and Strejilevich, 2004). Yet, WM tasks employed in EEG and MEG studies of neural oscillations have not included manipulation of mental representations and instead emphasized maintenance of visual stimuli. The aim of the present study was to identify abnormal neural oscillatory activity in schizophrenia during working memory by characterizing the timing, frequency, and cortical locations of neural responses elicited by a task that incorporated both maintenance and detailed analysis of visual objects of varying complexity. Our previous work has revealed that the Visual Object Construction (VOC) task used in the current study requires a participant to perform top-down spatial computations with visual information stored in WM (Chafee et al., 2005), thereby tapping encoding, maintenance, retrieval, and executive control functions.

We collected MEG data while participants performed the VOC task. The task required subjects to compare a visible object (abstract form composed of squares) to one stored in WM in order to identify a missing element (a single square). Neural ensemble recordings during the VOC task in nonhuman primates have demonstrated that the specific location of the missing element is coded in neural activity (Chafee et al., 2007, 2005; Crowe et al., 2008) and that the spatial computation is dissociated from sensorimotor control. In the present experiment we analyzed the time and frequency characteristics of neural oscillatory activity in cortical regions of interests (ROIs) computed through source localization of MEG using individualized realistic head models. The cortical ROIs underlying the visual WM system were chosen based on a functional magnetic resonance imaging (fMRI) study where blood-oxygen-level-dependent (BOLD) signal data were collected with the same visual WM task from the same subjects, and brain regions with WM-load dependent BOLD signal changes were identified (Kang et al., 2011). With the novel WM task and integration of multimodal neuroimaging data, we were able to identify abnormal neural oscillatory processes in schizophrenia as well as their neuroanatomical locations, demonstrating specific oscillatory deficits during encoding, maintenance, and retrieval processes within WM.

2. Methods

2.1. Participants

Twelve PSZ and thirteen age and gender matched non-psychiatric healthy control (HC) subjects participated in the study (see Table 1 for the demographic and clinical characteristics of the participants). Details of participant recruitment, clinical diagnosis, and exclusion criteria are described elsewhere (Kang et al., 2011). In brief, all patients met DSM-IV criteria for schizophrenia and were clinically stable outpatients. All patients but one had been prescribed antipsychotics at the time of testing. All participants were right-handed, except one control subject. We assessed current symptomatology using the Scale for the Assessment of Negative Symptoms (SANS; Andreasen, 1983a) and the Scale for the Assessment of Positive Symptoms (SAPS; Andreasen, 1983b) with PSZ, as well as the 24-item version of the Brief Psychiatric Rating Scale (BPRS; Lukoff et al., 1986) for PSZ and HCs. All patients were treated with antipsychotic medications. The medication dosage was quantified as Chlorpromazine (CPZ) equivalent score following the formula developed by Andreasen et al. (2010), and used to test if neural synchrony measures were correlated with antipsychotic medication. All participants gave an informed consent before they participate in the study. The study protocol was approved by the Institutional Review Boards of the VA Medical Center and the University of Minnesota.

2.2. Task and procedure

As part of an MEG session participants completed a visual object construction (VOC) task that had been developed to study spatial cognitive processing in the parietal cortex of nonhuman primates (Chafee et al., 2007, 2005; Crowe et al., 2008) and involved the encoding, maintenance, and retrieval of visual information (see Fig. 1a). The VOC task is based on tests of spatial cognitive function requiring the analysis of spatial locations of elements that make up an abstract visual object (Benton, 1967; Black and Strub, 1976;

Table 1
Demographic and clinical characteristics of subjects.

	Schizophrenia Patients (N = 12)	Controls (N = 13)	Statistics[a]
Demographic variables			
Age (years)	45.3 (10.8)	46.2 (7.7)	−0.24
Education (years)	13.8 (2.3)	16.8 (3.8)	−2.31*
Parental education (years)	13.7 (2.8)	12.5 (2.6)	1.04
IQ estimate	94.9 (13.2)	113.4 (10.6)	−3.98*
% Male	83%	76%	0.16
Clinical variables			
Overall symptomatology[b]	44. 7 (9.4)		
Psychosis symptom score[c]	1.9 (1.5)	–	–
Negative symptom score[d]	1.7 (0.9)	–	–
Disorganization symptom scores[e]	2.3 (1.4)	–	–
Illness duration (years)	24.8 (11.0)	–	–
Treatment variables			
Medication (CPZ equivalent)	641. 7 (445.1)	–	

Note: Values are mean and standard deviation unless otherwise noted.
IQ was estimated using scores on the Vocabulary and Block Design Subtests of the WAIS-III.
[a] $t_{(23)}$ for continuous variables and $\chi^2_{(1)}$ for a discrete variable (i.e., % Male).
[*] Indicate significant group difference.
[b] Overall symptomatology score was computed as a total BPRS score (range: 24–168).
[c] Psychosis symptom score was computed as the average global score for hallucinations and delusions in SAPS (range: 0 [none]–5 [severe]).
[d] Negative symptom score was computed as the average global score for alogia, affective flattening, avolition-apathy, and anhedonia-asociality in SANS (range: 0 [none]–5 [severe]).
[e] Disorganization symptom score was the global score for positive formal thought disorder in SAPS (range: 0 [none]–5 [severe]).

Driver et al., 1994; Driver and Halligan, 1991; Piercy et al., 1960). In order to complete the task participants were instructed to fixate their eyes on a dot as the center of the screen. Then an abstract object composed of contiguous squares (i.e., model) was displayed for 300 ms. Next, there was a delay period of either 1 or 5 s during which participants needed to maintain the object in memory. After the delay, an incomplete version of the object was presented (i.e., partial copy) that was missing a single square. After the partial copy of the object had been visible for 0.75 s, a pair of choice squares appeared to the left and right of the partial copy of the object. Participants pressed the left or right response key to indicate whether the addition of the corresponding left or right square formed the original object (i.e., model) when moved inward to be contiguous with the other squares. Thus, selection of the correct square was required to form the model visual object. The probability of a missing square on the left or right side was equal (i.e., 0.5). We parametrically manipulated visual WM load by varying the number of square elements that composed the model objects. Objects were constructed on a 5 × 5 grid of possible square locations. Each object included a 'frame' of squares filling the central column and base row of the grid, to which either two, four, or six contiguous squares were added at random locations (corresponding to the simple, intermediate, and complex spatial conditions, respectively). With the additional manipulation of the delay period there were a total six conditions defined by the three levels of complexity and two delay conditions (1 and 5 s). These six trial conditions were pseudo-randomly presented to participants during the MEG recording. The task ran until a participant achieved 40 correct

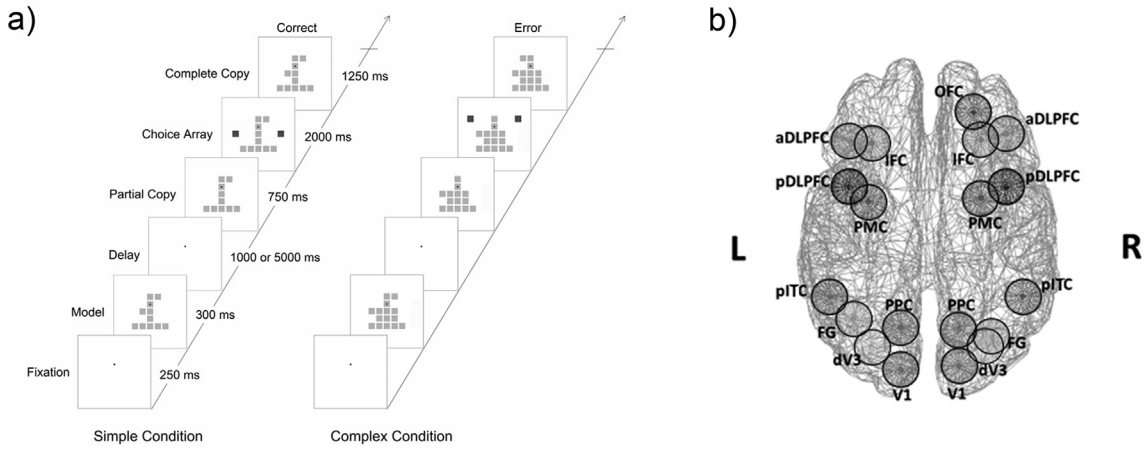

Fig. 1. Trial structure for the visual object construction (VOC) task (Chafee et al., 2005) and cortical regions showing VOC working memory (WM) complexity effects (Kang et al., 2011). (a) The VOC task was used to assess WM. Participants were required to encode a model object, maintain the object in working memory during a delay, and when presented with a partial copy of the model object indicate the location of the missing square element by selecting one of two choice squares to complete the model object. The delay period between model and partial copy objects within each trial was either 1 or 5 s. The simple complexity condition consisted of stimuli with two square elements added to an inverted T-shaped frame of squares (left). The complex stimulus condition involved six square elements added to the frame (right). See text for additional details of the VOC task. (b) Nineteen visual WM regions of interest (ROIs) depicted in top view of brain. These ROIs were identified through a magnetic resonance imaging (MRI) study in which the same subjects performed the VOC task during scanning. Abbreviations: DLPFC: dorsolateral prefrontal cortex, PMC: premotor cortex, IFC: inferior frontal cortex, OFC: orbitofrontal cortex, PPC: posterior parietal cortex, pITC: posterior inferior temporal cortex, FG: Fusiform Gyrus, dV3: dorsal V3, V1: primary visual cortex. The suffiixes 'a', 'p', and 'd' stand for 'anterior', 'posterior', and 'dorsal' locations of the ROIs, respectively.

trials in each of the simple, medium, and complex conditions (i.e., 60 correct trials in each of the short and long delay conditions) in order to have enough correct trials for time-frequency analysis.[1] Task performance was measured by mean reaction time (RT) and accuracy (i.e., number of correct trials divided by the number of total trials).

2.3. MEG data collection and preprocessing

MEG data was collected using a 248-sensor axial gradiometer MEG system (Magnes 3600WH, 4D-Neuroimaging, San Diego, CA, USA), located within an electromagnetically-shielded room. Data were acquired with 1017 Hz sampling rate. Eye movements were recorded at the same rate using horizontal and vertical electrooculograms (HEOG and VEOG). EOG electrodes were placed above and below the right eye and to the outer ocular canthi. The sensor configuration and head positions were obtained using a 3-D digitizer (Polhemus, Colchester, VT). Participants were asked to remain still during the task and movement was monitored with five signal coils placed on the participants head, digitized prior to MEG acquisition, and activated before and after data acquisition in order to monitor the participant's head position. Head position change was always less than 4 mm. MEG data processing and analysis procedures were conducted using Matlab (The MathWorks, Inc. Natick, MA, USA).

We applied a high-pass (0.5 Hz) and low-pass (256 Hz) filters to the MEG data and down-sampled recordings to 256 Hz using a Matlab anti-aliasing resample function. MEG signals were then segmented into epochs defined by model and partial-copy versions of visual object stimuli. For epochs pertaining to the model object data were segmented from −600 to 1600 ms for short-delay trials and −600 to 4600 ms for long-delay trials with 0 ms set to stimulus onset. For the partial-copy of the object stimulus data were segmented into epochs extending from −100 to 2100 ms relative to stimulus onset. Independent component analysis (ICA; Hyvärinen, 1999; Hyvärinen and Oja, 2000) was used to remove signal artifacts from various physiological and environmental sources (see Supplementary Material for details of ICA procedure), including eye-movements, heart signals, muscle artifacts (McMenamin et al., 2010) and microsaccades (Yuval-Greenberg et al., 2008). Unstable MEG sensors identified through visual inspection and the ICA procedure were excluded from cortical source signal computations.

2.4. Cortical source signal computation

To create MEG-derived estimates of the neural activity within cortical sources relevant to visual working memory functions elicited by the VOC task, we identified 19 cortical ROIs (see Fig. 1b and Supplementary Table 1) that showed increases in BOLD signal related to WM load in the VOC task (i.e., object complexity) for patients and control participants included in the present report (Kang et al., 2011).[2] Individual cortical surface models were created from T1-weighted structural MRI data using a FreeSurfer automated analysis pipeline (Fischl et al., 2002; http://ftp.nmr.mgh.harvard.edu/), and a boundary element method (BEM) was applied to create head models for the forward calculation of the magnetic field at the scalp. We applied a minimum norm algorithm (Dale and Sereno, 1993) to solve the inverse problem when computing source signals. Further details of the cortical source computation procedure for the 19 ROI's are presented in the Supplementary Material.

2.5. Time frequency distribution of cortical source neural oscillations

This study computed time-frequency (TF) energy of cortical source signals with Cohen's class TF transformation algorithm (Cohen and Leon, 1995) with reduced interference distribution (RID) method that provides uniform time-frequency resolution (Bernat et al., 2005) using a binomial time-frequency distribution (TFD) kernel (Jeong and Williams, 1991). To reduce data size without loss of temporal precision of oscillatory activity, single-trial TFD energy data were down-sampled from 256 Hz to 50 Hz and then averaged by task conditions (Cohen, 2014). TFDs were averaged across trials to separately test the effects of complexity and delay (see Supplementary Material for details of TFD analysis). The TFD energy for the model and the partial-copy periods of the object were normalized to represent percent signal change compared to the median TF energy for each frequency within a prestimulus baseline period (−500 to 0 ms relative to stimulus onset).

2.6. Statistical analysis

Response accuracy and reaction time were analyzed using a mixed repeated measures ANOVA with group (HC and PSZ) as a between subjects factor and complexity (simple, medium, and complex) and delay (short and long) as within subjects factors. Only correct trials were used in the analysis of RT. The TF energy of cortical sources had distinct features in the encoding (i.e., model; Fig. 2), maintenance (i.e., delay; Fig. 3), and retrieval/response (i.e., partial copy/choice array; Fig. 4) periods. The activity of cortical sources was quantified by averaging the energy within the time and frequency windows that were defined based on grand average TF surface for each group (Kriegeskorte et al., 2009). Mixed repeated-measures multivariate ANOVAs were conducted to test effects of group (HC and PSZ), ROI (cortical region), and the visual WM conditions of complexity (simple, medium, and complex) and delay (short and long). Analyses of the beta ERD component during the long-delay maintenance period also included a within subjects factor of Time which consisted of seven 0.5 s time-segments from 1 to 4.5 ms after model stimulus onset. Huynh-Feldt correction (Huynh and Feldt, 1976) was applied when the sphericity assumption was violated. Significant effects in the MANOVA were examined through appropriate follow-up tests (i.e., *t*-tests and repeated measures ANOVAs). We also examined relationships of TF-energy components with WM task performances and clinical symptom severity variables using Pearson correlation analyses. To limit Type I error in the correlation analyses, a false discovery rate (FDR; Benjamini and Hochberg, 1995; Ventura et al., 2004) correction with criterion levels of $p = 0.05$ and $q = 0.05$ was applied to *p*-values derived from the 19 ROIs.

3. Results

3.1. Behavioral performance

Analyses of how accurately participants were able to identify the square missing from the partial copy object (Fig. 1a) revealed main effects of group ($F_{(1,23)} = 12.01$, $p = 0.002$) and stimulus com-

[1] With this MEG session design, some patients had longer MEG recordings with more total trials than healthy control subjects. Two patients failed to respond on many later trials which resulted in them having chance-level accuracy on the task since performance was calculated by the number of correct trials divided by the total number of trials. Because MEG data were analyzed for correct trials which mostly came from early in the task prior to the two subjects drifting into nonresponding, and exclusion of the two subjects minimally affected results, findings were not dependent on data obtained from these two individuals. See Supplementary Material for analyses regarding these two subjects.

[2] The VOC task used in the fMRI study was identical with the one used in the MEG recording, except that the fMRI version VOC task had only single delay condition (1 s between model and partial-copy stimuli) and that the model stimulus duration was 750 ms in the fMRI study. In addition, 2 control subjects in the present study were not included in the fMRI study due to the poor quality of their fMRI data.

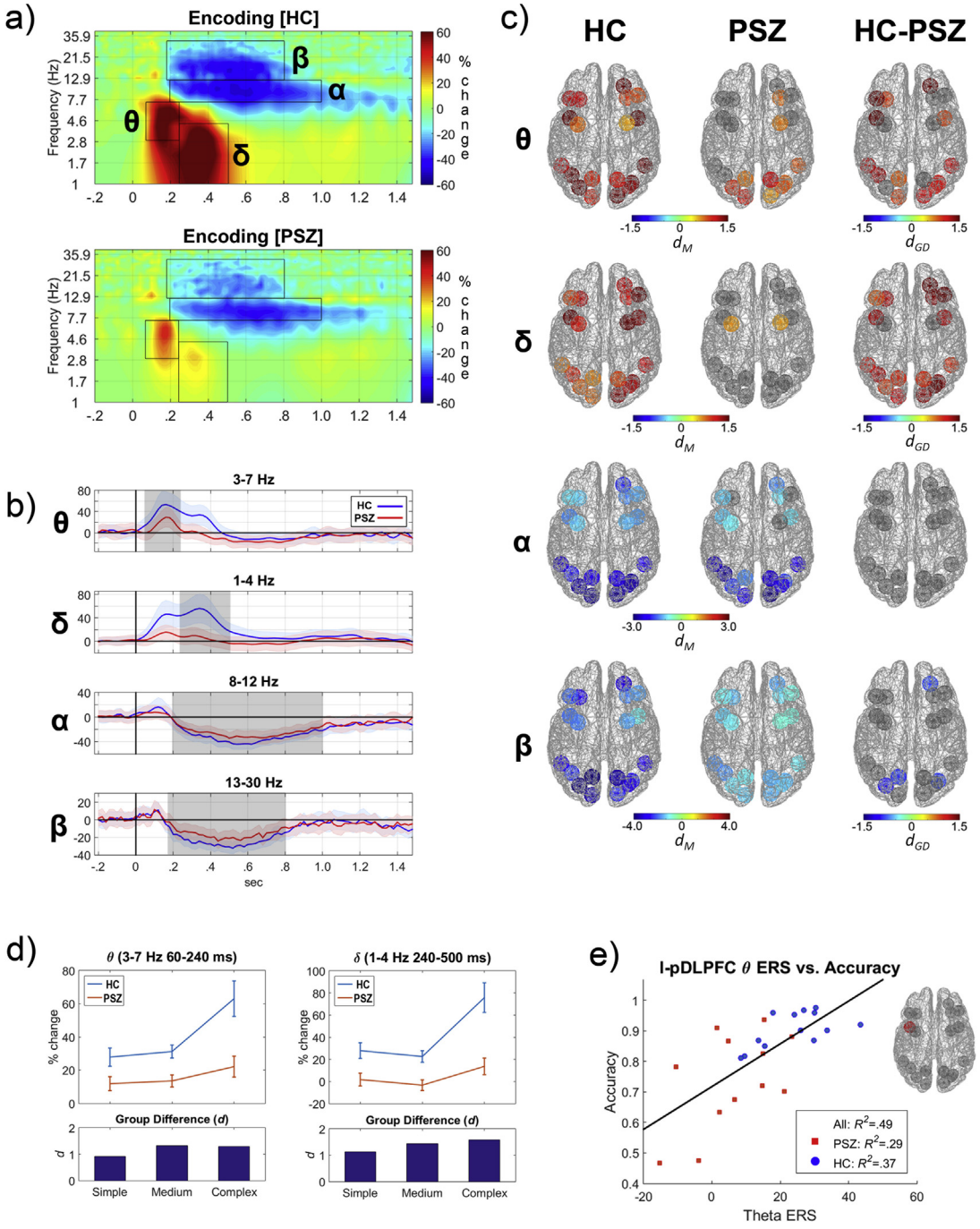

Fig. 2. Cortical oscillatory activity during encoding of the model object into working memory. Panels depict cortical source oscillatory activity in terms of time-frequency (TF) energy during the encoding of the model object into visual WM. (a) Grand average TF distribution of cortical oscillatory energy in HCs (top) and PSZ (bottom) collapsed across ROIs and task conditions. Data are normalized to represent percent signal change compared to the median TF energy within each frequency for a pre-stimulus baseline period (−500 to 0 ms). Superimposed black rectangles represent TF windows used to quantify four salient components of oscillatory activity observed during model object encoding. The four components were event-related-synchronization (ERS) in theta (θ: 3–7 Hz in 60–240 ms) and delta (δ: 1–4 Hz in 240–500 ms) and event-related desynchronization (ERD) in alpha (α: 8–12 Hz in 200–1000 ms) and beta (β: 13–30 Hz in 180–800 ms). The same windows were used for HCs and PSZ. (b) Time courses of oscillatory energy of the θ, δ, α, and β bands during model object encoding that were averaged across all ROIs and conditions. Light shading around the time series represents the standard error of the frequency mean. The dark gray rectangles represent the time periods for the TF windows marked in panel 'a' and used to quantify activity. PSZ showed marked reductions in θ and δ ERS in the peak time-windows around 200 ms and 300 ms, respectively. They also had moderate β and little α ERD decreases in later time windows (200–1000 ms). (c) The magnitude of oscillatory responses in each cortical region for θ, δ, α, and β frequencies during encoding (ERS in hot colors, ERD in cool colors) for time windows designated in panels 'a' and 'b'. Strength of activity for HCs (left column) and PSZ (middle column) was measured by computing the Cohen's d effect size for TF energy relative to the baseline period (d_M). The Cohen's d effect size of group differences between HCs and PSZ (d_{GD}; right column) was also computed. Colored ROIs depict cortical regions showing significant task-related changes in oscillatory activity within group (left and center columns) or between group differences (right column). Only cortical regions with significant effects were displayed in color. PSZ had fewer ROIs with θ and δ ERS and exhibited diminished β ERD in three ROIs compared to HCs. (d) Interactions between group and model object complexity for θ (left) and δ (right) ERS in HCs and PSZ. Group difference in effect sizes (Cohen's d) for the three levels of model object complexity (bottom). PSZ showed smaller increases in θ and δ ERS with greater model object complexity. (e) Scatter plot of the association between θ ERS for the left posterior DLPFC (l-pDLPFC) and VOC task performance accuracy on all trials. Individuals who had greater θ ERS in the l-pDLPFC during encoding had better WM performance.

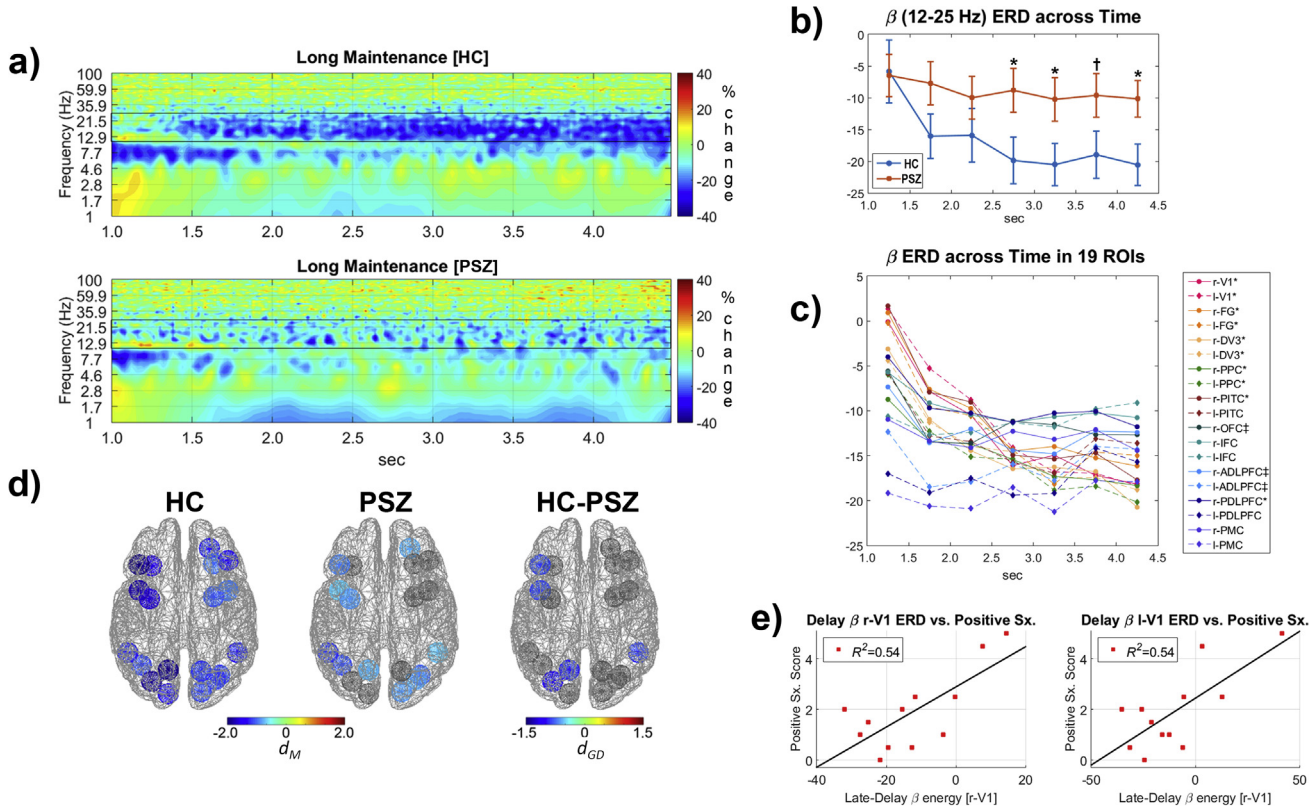

Fig. 3. Cortical oscillatory activity during the maintenance of the model object in working memory. Panels depict TF oscillatory energy during the maintenance of material in WM over a long-delay period from 1.0 to 4.5 s (i.e., period after the disappearance of model object stimulus). (a) Grand average TF energy of cortical oscillatory energy in HCs (top) and PSZ (botom) averaged across ROIs and complexity conditions and normalized to represent percent signal change compared to the median TF energy for each frequency within a pre-stimulus baseline (−500 to 0 ms relative to the model stimulus onset). Black rectangular outlines highlight frequencies of interest quantified for statistical analyses (β: 12–25 Hz). (b) Reduction in β oscillations in the HCs (top) during maintenance of material in WM was largely absent in PSZ (bottom). Examination of the interaction of group and time for β oscillation decreases (i.e., ERD) across seven 0.5 s time-intervals revealed smaller β ERD in PSZ, particularly in the late portion of the maintenance period (* = $p < 0.05$ and † = $0.05 < p < 0.10$) (2.5–3.0 s: $F_{(1,23)} = 4.75$, $p = 0.04$; 3.0–3.5 s: $F_{(1,23)} = 4.63$, $p = 0.04$; 3.5–4.0 s: $F_{(1,23)} = 3.37$, $p = 0.08$; 4.0–4.5 s: $F_{(1,23)} = 5.60$ $p = 0.03$). (c) Time course of β oscillations mean energy across seven 0.5 s intervals in the WM-related 19 ROIs. Regions with a significant ($p < 0.05$) linear decrease across time are marked with *, and those with a significant quadratic decrease (i.e., an early decrease followed by a leveling off at the end of the delay) are marked with ‡. Select visual, parietal, and prefrontal cortical regions exhibited greater β ERD over the course of the delay period. (d) Cortical regions where late-delay β ERD (11–25 Hz in 2.5–4.5 s) was most evident in HCs (left) and PSZ (middle), as well as group differences in the β oscillatory energy (right). (e) Scatterplots depicting a linear relationship between positive psychotic symptomatology and the late-delay β ERD for primary visual cortex (r-V1 and l-V1 ROIs). PSZ who had more positive psychotic symptoms tended to show less late delay β ERD (i.e., greater β energy).

plexity ($F_{(2,46)} = 29.30$, $p < 10^{-8}$) and a trend-level effect of delay period length ($F_{(1,23)} = 3.77$, $p = 0.06$), but no interactions. PSZ performed worse than HCs and accuracy worsened with more complex stimuli (Simple: PSZ: 0.83 ± 0.17; HC: 0.96 ± 0.04; Medium: PSZ: 0.73 ± 0.18; HC: 0.91 ± 0.08; Complex: PSZ: 0.69 ± 0.15; HC: 0.85 ± 0.07). Analyses of the reaction time for correct responses revealed main effects of group ($F_{(1,23)} = 6.72$, $p = 0.02$) and stimulus complexity ($F_{(2,46)} = 123.99$, $p < 0.001$) but no effect of delay period length ($F_{(2,46)} = 1.77$, *n.s.*). PSZ had longer reaction times than HCs and more complex stimuli resulted in slower responses (Simple: PSZ: 1.25 ± 0.26 s; HC: 1.04 ± 0.17 s; Medium: PSZ: 1.45 ± 0.26 s; HC: 1.22 ± 0.16 s; Complex: PSZ: 1.51 ± 0.26 s; HC: 1.33 ± 0.19 s). There was a trend-level group-by-delay interaction ($F_{(1,23)} = 3.49$, $p = 0.07$) which reflected PSZ having similar reaction times regardless of delay duration ($t_{(23)} = -0.35$, *n.s.*), while HCs had slower reaction times in the long compared to the short delay ($t_{(23)} = 2.25$, $p = 0.04$).

3.2. Cortical oscillations during encoding

Several notable neural responses of varying frequency and timing were observed when participants encoded the model object into visual WM (see Fig. 2). An early theta ERS (3–7 Hz and 60–240 ms) was observed in all ROIs in HCs, especially in posterior visual regions, bilateral pDLPFC, and right OFC. The theta response was greatly reduced in PSZ, in both frontal and posterior ROIs (see Fig. 2 panels a, b, and c). Analyses yielded main effects of group ($F_{(1,23)} = 13.73$, $p = 0.001$), object complexity ($F_{(1.8,41.1)} = 12.21$, $p = 10^{-4}$), and ROI ($F_{(8.8,203.3)} = 7.26$, $p < 10^{-8}$) indicating that the early theta oscillations during encoding varied across brain regions, was enhanced for more complex visual stimuli (complex > intermediate; $t_{(24)} = 3.26$, $p = 0.003$; intermediate vs simple; $t_{(24)} = 0.69$, *n.s.*), and were less evident in PSZ (Fig. 2, panel d). Supporting these observations were group-by-complexity ($F_{(1.8,203.3)} = 3.81$, $p = 0.035$) and complexity-by-ROI ($F_{(20.7,476.0)} = 2.36$, $p = 0.001$) interactions. Follow-up tests revealed that the increased encoding demands of more complex objects resulted in a greater theta ERS in HCs ($F_{(1.5,17.5)} = 11.85$, $p = 0.001$), but no such increase was evident in PSZ ($F_{(1.5,17.5)} = 1.71$, *n.s.*). Group differences in theta ERS were observed in many ROIs but were largest in the left DLPFC and the right OFC (see Fig. 2 panel c, and Supplementary Table 2 for effects at specific ROIs). Thus, PSZ not only had a reduced theta ERS in dorsolateral prefrontal and orbital frontal brain regions, but also a failure to modulate the ERS in these cortical areas in response to greater encoding demands. Better performance on the VOC task was predicted by greater encoding theta ERS in the left pDLPFC

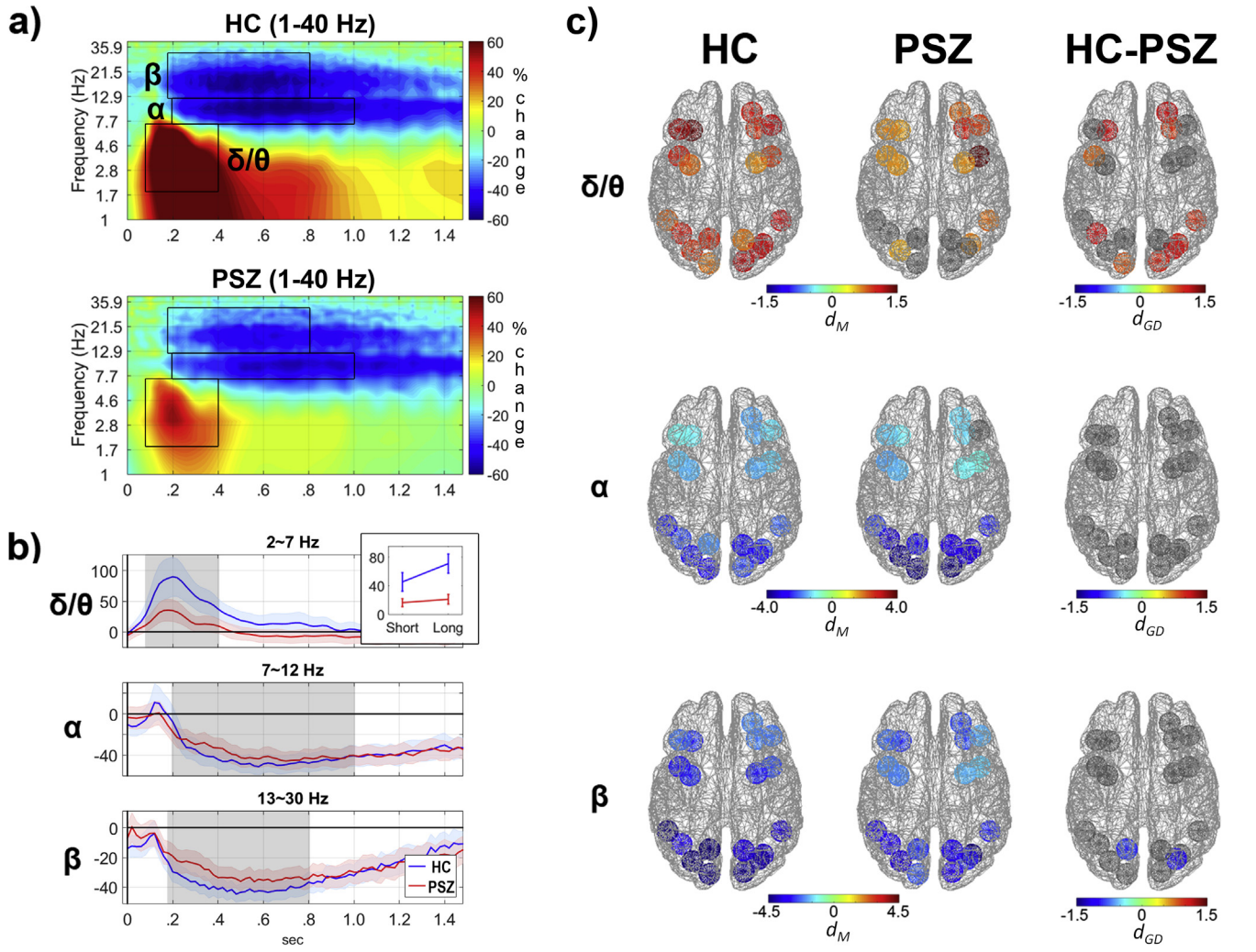

Fig. 4. Cortical oscillatory activity on retrieval of material from working memory during viewing of the partial copy object stimulus. Data reflect oscillatory activity in cortical regions time-locked to the onset of the partial copy of the object stimulus (0 s in panels a and b). (a) Grand average TF distribution of cortical oscillatory energy in HCs (top) and PSZ (bottom) collapsed across ROIs and conditions and normalized to represent percent signal change compared to the median TF energy for each frequency within a pre-stimulus baseline period (−500–0 ms). Three TF components quantified for statistical analyses are depicted by black rectangles; θ/δ (2–7 Hz in 80–400 ms), α (8–12 Hz in 200–1000 ms), and β (13–30 Hz in 180–800 ms). (b) Time course of oscillatory energy of the δ/θ, α, and β frequency bands during retrieval of material from WM that were averaged across all ROIs and conditions. During the retrieval of material PSZ had a large reduction in θ/δ ERS and a modest reduction in β ERD compared to HCs. As depicted in the inset, deficits in θ/δ ERS for PSZ were most evident in trials with long delay periods preceding retrieval. (c) The magnitude of oscillatory responses for cortical regions in δ/θ, α, and β bands in HCs (left) and PSZ (middle) during retrieval of material from WM in response to the partial copy object stimulus. PSZ had reductions in δ/θ ERS in the prefrontal and ventral visual cortical regions, as well as reduced β ERD in the left PPC and the right dV3.

($r_{(24)} = 0.70$, $p = 10^{-4}$, FDR-adjusted $p = 0.002$; see Fig. 3e) and the right OFC ($r_{(24)} = 0.53$, $p = 0.007$, FDR-adjusted $p = 0.067$) across subject groups.

Similar to theta activity, delta oscillations (1–4 Hz and 240–500 ms) increased in all ROIs during encoding of the object stimulus for HCs, particularly in the prefrontal and posterior ROIs of the right hemisphere. In PSZ delta oscillations largely failed to increase during encoding. The delta response at encoding showed main effects of group ($F_{(1,23)} = 16.20$, $p = 0.001$) and model object complexity ($F_{(1.6,36.8)} = 25.07$, $p < 10^{-7}$), but not ROI ($F_{(7.4,169.5)} = 1.40$, *n.s.*). More complex visual stimuli elicited greater delta ERS (complex > intermediate; $t_{(24)} = 4.85$, $p < 10^{-4}$; intermediate vs. simple; $t_{(24)} = -1.48$, *n.s.*) across cortical regions, and PSZ showed less delta activity than HCs at most cortical regions (right column Fig. 2c). In addition, there was an interaction of group with complexity ($F_{(1.8,203.3)} = 3.81$, $p = 0.035$), which was due to larger complexity-dependent delta ERS modulation in HCs ($F_{(1.6,19.5)} = 19.83$, $p < 10^{-4}$) compared to PSZ ($F_{(1.6,17.1)} = 6.88$, $p = 0.010$; see Fig. 2d and Supplemental Table 2).

Reductions in alpha frequencies (i.e., ERD; 8–12 Hz and 200–1000 ms) were prominent in most cortical regions in both groups during model object encoding. Analyses only revealed a main effect of ROI ($F_{(10.7,246.1)} = 21.83$, $p < 10^{-29}$) reflecting that alpha ERD was larger in posterior than prefrontal regions. Beta (13–30 Hz and 180–800 ms) ERD was also most evident in posterior visual regions (ROI: $F_{(10.2,235.4)} = 11.78$, $p < 10^{-15}$). PSZ had less beta ERD than HCs (group: $F_{(1,23)} = 4.98$, $p = 0.036$) especially in the right OFC and the posterior visual cortices (see Fig. 2c). There were no effects of stimulus complexity or interactions for beta ERD.

3.3. Cortical oscillatory activity during maintenance of material in working memory

When material was maintained in WM during the delay period, sustained beta ERD was evident. Specifically, a beta (12–25 Hz) ERD was observed from 1.0 to 4.5 which was after the disappearance of the model object stimulus. Beta ERD was clearly discernable in HCs but weak in PSZ (see Fig. 3 panels a & b). Statistical

tests revealed that the beta (12–25 Hz) ERD became greater over the delay period (Time $F_{(3.0,69.5)} = 8.64$, $p < 10^{-4}$) and varied across cortical regions (ROIs $F_{(10.8,248.8)} = 2.00$, $p = 0.03$) with ROI interacting with Time ($F_{(23.7,545.8)} = 4.35$, $p < 10^{-10}$; Fig. 3c). It was found that the visual, posterior parietal, and dorsolateral prefrontal cortices (PPC and DLPFC ROIs) had either linear or quadratic decreases in the beta energy (i.e., greater ERD) across time, while other prefrontal ROIs tended to have stable beta ERD during maintenance. The group difference for the entire time-window was not significant ($F_{(1,23)} = 2.75$, *n.s.*) but there was a group-by-time interaction ($F_{(3.0,69.5)} = 3.47$, $p = 0.02$), consistent with group differences in the beta ERD being greatest in later time-windows (2.5–4.5 s), especially in the left DLPFC, PPC, dV3, and the right pITC (Fig. 3 panels d). Individuals in the PSZ group who showed less beta ERD in primary visual cortex (V1) tended to show more positive symptoms of schizophrenia (r-V1: $r_{(11)} = 0.73$, $p = 0.006$, FDR-adjusted $p = 0.042$; l-V1: $r_{(11)} = 0.74$, $p = 0.006$, FDR-adjusted $p = 0.042$; see Fig. 3e).

3.4. Cortical oscillatory activity during retrieval of material from working memory

When the partial copy object was presented and the participant needed to contrast the partial copy with the model object stimulus stored in working memory in order to select the correct missing element (i.e., "Choice Array" in Fig. 1), cortical regions showed theta, delta, alpha, and beta oscillatory responses similar to those observed when the model object stimulus was initially encoded (see Fig. 4). The early increases in delta and theta energy (i.e., delta/theta ERS) in the retrieval period was observed in most cortical regions, but the strength varied across areas as indicated by a main effect of ROI, $F_{(5.9,135.9)} = 2.71$, $p = 0.017$. HCs had strong delta/theta ERS especially in anterior prefrontal cortical areas (i.e., aDLPFC, IFC, and OFC) and visual regions of the right cerebral hemisphere (top row of panel c in Fig. 4). The delta/theta ERS was larger for trials with long delay maintenance periods than short delay periods ($F_{(1,23)} = 21.29$, $p = 10^{-4}$), but not different across complexity levels ($F_{(2,46)} = 0.91$, *n.s.*), perhaps indicating greater retrieval demands when material was maintained in WM for longer periods (Fig. 4 panel b). PSZ had smaller delta/theta ERS than HCs ($F_{(1,23)} = 7.23$, $p = 0.01$) especially in the anterior prefrontal and posterior cortical regions of the ventral visual pathways. Additionally, group interacted with delay ($F_{(1,23)} = 10.06$, $p = 0.004$) and follow-up tests showed that the delay effect was strong in HCs ($F_{(1,12)} = 23.89$, $p < 0.001$) but absent in PSZ ($F_{(1,11)} = 1.54$, *n.s.*). For HCs the group effect was marginal for the short delay ($F_{(1,23)} = 3.94$, $p = 0.06$) but more notable for the long delay ($F_{(1,23)} = 10.44$, $p = 0.004$). Like the encoding period, alpha and beta frequency ERD were observed from about 200 ms after the partial-copy object onset, especially in the posterior visual regions (ROI effect in alpha ERD: $F_{(8.8,203.0)} = 22.25$, $p < 10^{-25}$; ROI effect in beta ERD: $F_{(8.9,204.5)} = 19.78$, $p < 10^{-22}$). Alpha ERD (8–12 Hz in 200–1000 ms) had neither group nor condition effects. Beta ERD (13–30 Hz in 180–800 ms) was reduced in PSZ compared to HCs (Group: $F_{(1,23)} = 4.37$, $p = 0.048$), with the group difference being more evident in the left PPC and the right dV3 that was independent of stimulus complexity and length of the delay maintenance period.

Cortical regions showed increased gamma energy (ERS) during retrieval of material from WM in response to the partial copy stimulus (46–100 Hz from 100 to 800 ms after partial copy stimulus onset). Gamma ERS was much larger during retrieval than encoding ($F_{(1,24)} = 79.90$, $p < 10^{-8}$), especially in parietal, visual, and premotor cortices (Phase × ROI: $F_{(10.4,239.4)} = 5.97$, $p < 10^{-7}$; see Fig. 5a). As such, gamma ERS may reflect neural computations that take place during the retrieval of material from WM that do not take place during encoding processes of the model period. One process unique to the partial copy stimulus period in the VOC task is localization of the missing square compared to the model object encoded into WM. These spatial localization processes have been related to activation of single neurons in posterior parietal cortex (Chafee et al., 2007, 2005; Crowe et al., 2008). It is noteworthy that gamma ERS varied across cortical regions (ROIs $F_{(10.8,247.9)} = 10.81$, $p < 10^{-15}$), with large gamma responses in the PPC consistent with cellular recordings (Chafee et al., 2007, 2005; Crowe et al., 2008). Gamma ERS increases during retrieval were also evident in bilateral PMC and regions of dorsal visual pathways including dV3, and V1. Nonetheless, there failed to be a main effect of group ($F_{(1,23)} = 1.55$, *n.s.*) and only a trend-level interaction of group with ROI ($F_{(10.8,247.9)} = 1.73$, $p = 0.070$). The gamma ERS was not different across WM conditions of stimulus complexity and delay length. The absence of such effects is consistent with PSZ having intact spatial computational processes but deficient encoding and retrieval functions indicated by limited theta and delta ERS. Follow-up tests to explore the trend-level interaction revealed that PSZ had reduced gamma synchrony in the bilateral PMC (r-PMC: $F_{(1,23)} = 7.35$, $p = 0.012$.; l-PMC: $F_{(1,23)} = 8.51$, $p = 0.008$) and the right PPC ($F_{(1,23)} = 6.55$, $p = 0.018$; see Fig. 5b).

4. Discussion

We used time-frequency analyses of MEG-derived cortical source signals to investigate aberrations in neural oscillations in schizophrenia during a visual WM task. PSZ had deficits in early prefrontal theta frequency responses related to the encoding of material that were predictive of poor WM performance (Fig. 2). Similar low-frequency abnormalities were evident in PSZ when material was retrieved from WM (Fig. 4). PSZ also failed to sustain beta desynchronization during maintenance of material within WM (Fig. 3) and showed deficient gamma oscillations in posterior parietal and premotor cortices during retrieval of material (Fig. 5). Results of the current investigation suggest that although beta and gamma oscillatory deficits are evident during WM in schizophrenia, deficient theta activity in prefrontal cortex is the abnormal oscillatory response most predictive of impaired WM. Unlike previous studies that emphasized the role of visual cortical deficits in encoding failures in PSZ (Dias et al., 2011; Haenschel et al., 2007), the current finding demonstrated the critical role of prefrontal theta oscillations in visual encoding for WM and the deficits observed in PSZ.

4.1. Deficient cortical theta oscillations at encoding predict working memory impairment

During encoding of visual objects into WM the increase in theta oscillations (i.e., ERS from 3 to 7 Hz in 60–240 ms period after model stimulus onset) was observed in most prefrontal-posterior cortical regions, indicating that encoding not only required visual cortical processes but also prefrontal cortical activity. It has been hypothesized that theta oscillations enable encoding of multiple items into WM (Sauseng et al., 2010) and that these processes are impaired in schizophrenia (for a review see Lynn and Sponheim, 2016). The theta synchrony patterns were somewhat different between the visual and prefrontal cortical regions. Unlike visual cortical areas where theta frequencies increased with the complexity of the object encoded into WM, most prefrontal regions failed to show object complexity-dependent theta activity increases. It is possible that theta frequency oscillations are necessary for efficient encoding of visual information and that this is facilitated by synchronous activity in prefrontal and visual cortical regions (Bar et al., 2006). The current investigation revealed that

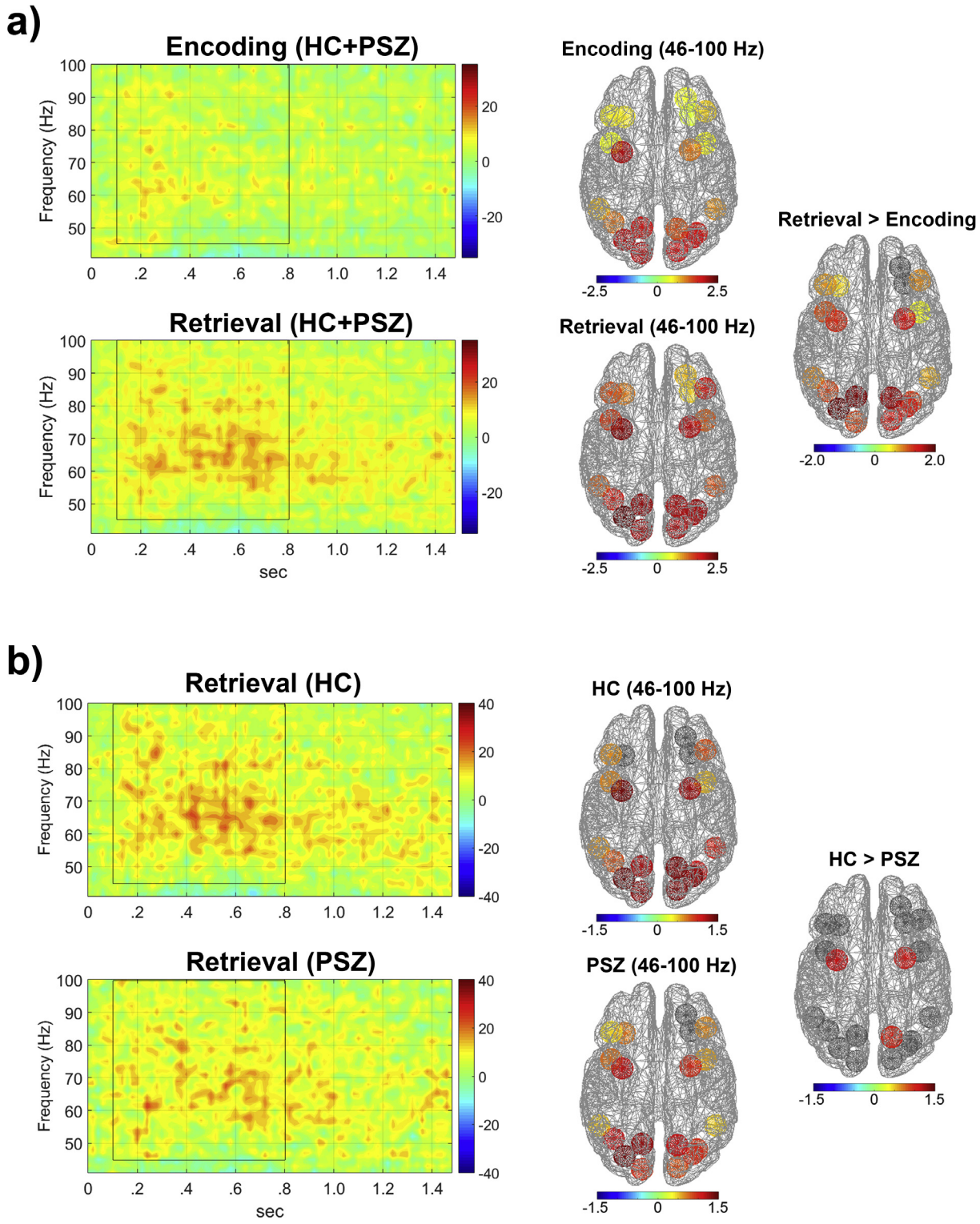

Fig. 5. Gamma frequency activity during encoding and retrieval of material from working memory. Panels depict TF energy of high frequency (gamma) cortical oscillatory energy in WM-related cortical regions. (a) TF energy of gamma (γ) oscillations during encoding (model object) and retrieval (partial copy of model object) for PSZ and HC groups averaged across all 19 ROIs and all conditions. The energy of γ frequencies was quantified as percent change in activity within windows of 46–100 Hz and 100–800 ms (marked by black rectangular outline) relative to a −500 to 0 ms pre-stimulus period. Cortical regions (right) showing significant increases in γ activity depicted in terms of Cohen's *d* effect sizes for within group differences during encoding and retrieval (d_M) and between encoding and retrieval phases (d_P). The γ oscillatory energy was larger during retrieval than in the encoding period, and was most evident in bilateral posterior parietal cortex (PPC), premotor cortex (PMC), as well as dorsal visual ROIs. (b) TF energy of γ oscillations during retrieval of material from WM in HCs (top) and PSZ (bottom) measured by percent change from the prestimulus baseline and averaged across all 19 ROIs and all conditions. PSZ had diminished γ energy in the bilateral PMC and the right PPC on retrieval of information from WM.

impaired theta oscillatory responses in PSZ were greatest in the left DLPFC and the right OFC, supporting the notion that in schizophrenia a failure in prefrontal facilitation of visual cortical processes may partially explain WM deficits in the disorder. The early theta frequency response at encoding was accompanied by an object complexity-dependent delta frequency response (1–4 Hz in 240–500 ms) that was deficient in PSZ compared to HCs. Recent work provides evidence that delta oscillations limit the interference of competing stimuli during attention through synchronization of neural activity distributed across cortical networks that include prefrontal cortex (see Harmony, 2013 for review). As delta-theta coupling might facilitate cortical interlaminar interaction and memory consolidation (Carracedo et al., 2013), the theta-delta ERS sequence might represent a similar neurocognitive process of prefrontal-visual top-down processing of visual stimuli for encoding.

4.2. Absence of beta desynchronization during maintenance of material in working memory in schizophrenia

Analysis of cortical source signals revealed that during the delay period (1.0–4.5 s after model-stimulus onset) when encoded material needed to be maintained in WM, PSZ failed to show desynchronization of oscillations in the beta frequency range (12–25 Hz). The beta desynchronization we observed in HCs during maintenance is consistent with findings from other studies that have used MEG-based indices to characterize neural processes underlying maintenance functions during a visuospatial delayed saccade task (Medendorp et al., 2007) and a delayed matching-to-sample task (Palva et al., 2011). Hanslmayr et al. (2012) proposed the "information by desynchronization" hypothesis, which postulates that a certain degree of beta and alpha desynchronization is necessary for successful memory encoding, maintenance, and retrieval. The beta ERD that we observed over the long-delay period might represent such a desynchronization in the prefrontal-parietal executive control network, and may support the maintenance of internal representations of visual objects.[3] The time-dependent beta ERD increases in the DLPFC-PPC along with the visual cortices might represent cortical oscillatory mechanisms of top-down modulation of sensory cortices for maintenance. Importantly, maintenance-related beta desynchrony was most limited in PSZ in regions central to the executive control network (i.e., dorsolateral prefrontal and posterior parietal cortices). Also, deficiencies in the late-delay beta ERD in primary visual cortex predicted positive symptoms in schizophrenia highlighting how beta oscillatory abnormalities that extend beyond the executive control work may be important to understanding psychotic symptomatology. Abnormal sensory cortical beta ERD during absence of actual stimuli might contribute to generation of positive symptoms like hallucinations.

4.3. Re-emergence of deficient low frequency oscillations in schizophrenia at retrieval

Deficient low frequency responses (delta/theta: 2–7 Hz in 100–460 ms) were observed in prefrontal and posterior brain regions in PSZ when material was retrieved from WM. In contrast to the encoding period theta response that was modulated by the complexity of visual object, the response during retrieval was larger for a preceding long delay maintenance period as compared to a short delay period. Theta oscillations at retrieval may reflect the updating of WM representations (Itthipuripat et al., 2013) and integrating of distributed brain functions associated with material in WM (Sauseng et al., 2010). PSZ failed to show delay-related modulation of low frequency responses in anterior prefrontal cortex and visual cortices within ventral visual pathways consistent with deficient retrieval and possible impairments in updating the contents of WM. Additionally, PSZ had reduced beta desynchronization in areas of the dorsal visual pathway (i.e., PPC and dV3) during retrieval. These beta desynchrony deficits may reflect difficulty reactivating visual memory traces of the model object (Burgess and Gruzelier, 2000; Khader and Rösler, 2011).

4.4. Gamma frequency ERS deficits in PSZ during retrieval and manipulation

PSZ also demonstrated a tendency toward having limited gamma frequency responses during retrieval (gamma ERS, 46–100 Hz in 100–800 ms period) that was evident in parietal and premotor cortices. Importantly, gamma oscillations were generally greater at retrieval than encoding suggesting that synchronous gamma oscillatory activity was recruited with the requirement to localize a missing element in the partial copy of the object stimulus. The possibility that the gamma response reflects spatial localization processes carried out in parietal cortex is bolstered by cellular recordings within posterior parietal cortex during the VOC task showing that parietal neurons carry out the spatial computations required to identify the missing element in the partial copy object (Chafee et al., 2005). Also, evidence suggests that premotor cortical gamma activity may contribute more to the spatial manipulation of material in visual WM as compared to motor-planning (Mohr, 2006), which is consistent with our observation of deficient premotor gamma synchrony in PSZ occurring long before the motor response associated with selection of the choice square missing from the abstract object.

5. Conclusions

Analyses of cortical oscillatory activity during a visual WM task revealed that PSZ had abnormal synchronous neural responses in specific time-frequency oscillations of distinct cortical regions during encoding, maintenance, and retrieval of object stimuli. Schizophrenia was associated with markedly attenuated theta and delta responses in prefrontal cortex when an abstract object was encoded into WM. Deficient theta activity at encoding predicted worse performance accuracy on the WM task. PSZ also had maintenance-related synchrony deficits, as reflected by weaker beta desynchrony particularly during the late-delay period in patients. On retrieval of object information from WM, PSZ again demonstrated attenuated delta and theta responses, but additionally exhibited diminished gamma oscillations in parietal cortex which were likely reflective of spatial analysis of the partial copy object. Despite their substantial deficits in many ERS/ERD components, PSZ were able to perform the visual WM task above chance level even in the most difficult condition. Like people with prefrontal lesions, PSZ might perform the task relying on other intact neurocognitive processes perhaps represented by alpha and beta ERD within visual cortices during encoding and retrieval. Alpha and beta ERD may represent activity within a posterior cortical mechanism for the short-term maintenance of information (D'Esposito et al., 2006). Importantly, group differences in cortical oscillatory activity appear not to be the result of antipsychotic medication since no indices of oscillatory activity correlated with antipsychotic dosage equivalent scores. The present study had some limitations in that small samples were used, thus our

[3] Due to a limited number of trials in the long-delay condition WM−load effects could not be tested for the long-delay beta desynchrony. But in a supplementary analysis, it was found that the beta ERD in short-delay period (1200–1500 ms after model-stimuli-onset when the beta ERD firstly observed and enough number of trials were available) tended to increase according to the complexity level of visual stimuli ($F_{(1.8,42.2)} = 2.75$, $p = 0.080$).

statistical power to detect more subtle group differences or associations of ERS/ERD indices with performance and clinical variables may have been limited. The current findings should be replicated with larger samples.

Results of the present study have implications for neurobiological models of schizophrenia that describe how abnormal oscillations in neuronal populations lead to disruptions in cognitive functions such as WM. Recent experimental evidence points to how processes central to WM may be mediated through temporal interactions between cortical rhythms of low (theta and delta) and high (gamma) frequencies across a variety of cortical regions and involve the relative timing of oscillations (Carracedo et al., 2013; Roopun, 2008), and that such processes may underlie impairment in WM in schizophrenia (Lynn and Sponheim, 2016). Inhibitory interneurons may have crucial roles in modulating the temporal dynamics of neuronal rhythms, and abnormal cellular and molecular markers in PSZ suggest malfunction of cortical inhibitory interneurons in the disease (see Pittman-Polletta et al., 2015 for review). Intrinsic and synaptic feedback currents of various gamma-aminobutyric acid (GABA) ergic interneurons determine frequency of cortical rhythm and oscillatory dynamics by introducing inhibitory synaptic perturbations in varying temporal scales in N-methyl- D-aspartate receptor (NMDAR)-driven cortical networks (Lucy M. Carracedo et al., 2013; Rotstein et al., 2005; Vijayan and Kopell, 2012; Whittington et al., 2000). Mutations in schizophrenia susceptibility genes including disrupted in schizophrenia (DISC-1; Koyama et al., 2013) and dystrobrevin binding protein 1 (DTNBP1; Carlson et al., 2011) are known to alter neurodevelopmental trajectory so that cytoarchitecture and functions of inhibitory interneurons are affected. Cellular and molecular alterations in schizophrenia such as changes in GABAergic signaling, NMDA hypofunction, and dopaminergic dysregulation interact to alter cortical inhibitory dysfunctions (Uhlhaas and Singer, 2010), leading to aberrant cortical rhythms in low to high frequency. Therefore, the current findings of disrupted oscillatory dynamics in the prefrontal, parietal, and visual cortical networks appear to represent intermediate neural mechanisms relating genetic and cellular/molecular pathophysiology factors to deficits in multiple cognitive processes in PSZ. Future studies with larger samples and investigation of interregional neural synchronization in large-scale cortical networks will further elucidate nature of abnormal synchronous cortical networks in PSZ.

Acknowledgements

This work was supported by grants from the National Institutes of Mental Health (grant numbers: 5R24MH069675 (SRS), RO1MH77779, and R03MH106831 (SRS)), and by a grant from the Department of Veterans Affairs Clinical Science Research and Development Program (I01CX000227) to Dr. Scott Sponheim, as well as by the Mental Health Patient Service Line at the Veterans Affairs Health Care System, Minneapolis, Minnesota, US. We are grateful to the participants and also for the efforts of Rachel Force, John J. Stanwyck, Amy Silberschmidt, and JoAn Laes.

Conflict of interest

The author declares that the research was conducted in the absence of any commercial or financial relationships that could be construed as a potential conflict of interest.

Appendix A. Supplementary material

Supplementary data associated with this article can be found, in the online version, at https://doi.org/10.1016/j.clinph.2017.10.024.

References

Andreasen NC. Scale for the assessment of negative symptoms. Iowa City: University of Iowa; 1983a.
Andreasen N. The scale for the assessment of positive symptoms. Iowa City: University of Iowa; 1983b.
Andreasen NC, Pressler M, Nopoulos P, Miller D, Ho BC. Antipsychotic dose equivalents and dose-years: a standardized method for comparing exposure to different drugs. Biol Psychiatry 2010;67:255–62. https://doi.org/10.1016/j.biopsych.2009.08.040.
Bachman P, Kim J, Yee CM, Therman S, Manninen M, Lönnqvist J, et al. Abnormally high EEG alpha synchrony during working memory maintenance in twins discordant for schizophrenia. Schizophr Res 2008;103:293–7. https://doi.org/10.1016/j.schres.2008.04.006.
Baddeley AD. Working memory: theories, models, and controversies. Annu Rev Psychol 2012;63:1–29. https://doi.org/10.1146/annurev-psych-120710-100422.
Bar M, Kassam KS, Ghuman AS, Boshyan J, Schmid AM, Dale AM, et al. Top-down facilitation of visual recognition. Proc Natl Acad Sci 2006;103:449–54. https://doi.org/10.1073/pnas.0507062103.
Barch DM, Ceaser A. Cognition in schizophrenia: Core psychological and neural mechanisms. Trends Cogn Sci 2012;16:27–34. https://doi.org/10.1016/j.tics.2011.11.015.
Basar-Eroglu C, Brand A, Hildebrandt H, Karolina Kedzior K, Mathes B, Schmiedt C. Working memory related gamma oscillations in schizophrenia patients. Int J Psychophysiol 2007;64:39–45. https://doi.org/10.1016/j.ijpsycho.2006.07.007.
Benjamini Y, Hochberg Y. Controlling the false discovery rate: a practical and powerful approach to multiple testing. J R Stat Soc Ser B 1995;57:289–300. https://doi.org/10.2307/2346101.
Benton AL. Constructional apraxia and the minor hemisphere. Confin Neurol 1967;29:1–16. https://doi.org/10.1159/000103671.
Bernat EM, Williams WJ, Gehring WJ. Decomposing ERP time-frequency energy using PCA. Clin Neurophysiol 2005;116:1314–34. https://doi.org/10.1016/j.clinph.2005.01.019.
Black FW, Strub RL. Constructional apraxia in patients with discrete missile wounds of the brain. Cortex 1976;12:212–20.
Burgess AP, Gruzelier JH. Short duration power changes in the EEG during recognition memory for words and faces. Psychophysiology 2000;37:596–606. https://doi.org/10.1111/1469-8986.3750596.
Cannon TD, Glahn DC, Kim J, Van Erp TGM, Karlsgodt K, Cohen MS, et al. Dorsolateral prefrontal cortex activity during maintenance and manipulation of information in working memory in patients with schizophrenia. Arch Gen Psychiatry 2005;62:1071–80. https://doi.org/10.1001/archpsyc.62.10.1071.
Carlson GC, Talbot K, Halene TB, Gandal MJ, Kazi HA, Schlosser L, et al. Dysbindin-1 mutant mice implicate reduced fast-phasic inhibition as a final common disease mechanism in schizophrenia. Proc Natl Acad Sci USA 2011;108:E962–70. https://doi.org/10.1073/pnas.1109625108.
Carracedo LM, Kjeldsen H, Cunnington L, Jenkins A, Schofield I, Cunningham MO, et al. A neocortical delta rhythm facilitates reciprocal interlaminar interactions via nested theta rhythms. J Neurosci 2013;33:10750–61. https://doi.org/10.1523/JNEUROSCI.0735-13.2013.
Chafee MV, Averbeck BB, Crowe DA. Representing spatial relationships in posterior parietal cortex: Single neurons code object-referenced position. Cereb Cortex 2007;17:2914–32. https://doi.org/10.1093/cercor/bhm017.
Chafee MV, Crowe DA, Averbeck BB, Georgopoulos AP. Neural correlates of spatial judgement during object construction in parietal cortex. Cereb Cortex 2005;15:1393–413. https://doi.org/10.1093/cercor/bhi021.
Cohen L, Leon. Time-frequency analysis. Englewood Cliffs, NJ.: Prentice Hall PTR; 1995.
Cohen MX. Analyzing neural time series data: theory and practice. Cambridge, MA: The MIT Press; 2014. doi:https://doi.org/10.1017/CBO9781107415324.004.
Crowe DA, Averbeck BB, Chafee MV. Neural ensemble decoding reveals a correlate of viewer- to object-centered spatial transformation in monkey parietal cortex. J Neurosci 2008;28:5218–28. https://doi.org/10.1523/JNEUROSCI.5105-07.2008.
D'Esposito M, Cooney JW, Gazzaley A, Gibbs SEB, Postle BR. Is the prefrontal cortex necessary for delay task performance? Evidence from lesion and FMRI data. J Int Neuropsychol Soc 2006;12:248–60. https://doi.org/10.1017/S1355617706060322.
Dale AM, Sereno MI. Improved localization of cortical activity by combining EEG and MEG with MRI cortical surface reconstruction: a linear approach. J Cogn Neurosci 1993;5:162–76. https://doi.org/10.1162/jocn.1993.5.2.162.
Dias EC, Butler PD, Hoptman MJ, Javitt DC. ONLINE FIRST early sensory contributions to contextual encoding deficits in Schizophrenia. Arch Gen Psychiatry 2011;68:654–64. https://doi.org/10.1001/archgenpsychiatry.2011.17.
Driesen NR, Leung HC, Calhoun VD, Constable RT, Gueorguieva R, Hoffman R, et al. Impairment of working memory maintenance and response in schizophrenia: functional magnetic resonance imaging evidence. Biol Psychiatry 2008;64:1026–34. https://doi.org/10.1016/j.biopsych.2008.07.029.
Driver J, Baylis GC, Goodrich SJ, Rafal RD. Axis-based neglect of visual shapes. Neuropsychologia 1994;32:1353–6. https://doi.org/10.1016/0028-3932(94)00068-9.
Driver J, Halligan JC. Can visual neglect operate in object-centred co-ordinates? Cogn Neuropsychol 1991;8:475–96.

Erickson MA, Hahn B, Leonard CJ, Robinson B, Gray B, Luck SJ, et al. Impaired working memory capacity is not caused by failures of selective attention in schizophrenia. Schizophr Bull 2015;41:366–73. https://doi.org/10.1093/schbul/sbu101.
Fischl B, Salat DH, Busa E, Albert M, Dieterich M, Haselgrove C, et al. Whole brain segmentation: automated labeling of neuroanatomical structures in the human brain. Neuron 2002;33:341–55. https://doi.org/10.1016/S0896-6273(02)00569-X.
Gold JM, Hahn B, Zhang WW, Robinson BM, Kappenman ES, Beck VM, et al. Reduced capacity but spared precision and maintenance of working memory representations in schizophrenia. Arch Gen Psychiatry 2010;67:570–7. https://doi.org/10.1001/archgenpsychiatry.2010.65.
Haenschel C, Bittner R, Waltz J, Haertling F, Wibral M, Singer W, et al. Cortical oscillatory activity is critical for working memory as revealed by deficits in early-onset schizophrenia. J Neurosci 2009;29:9481–9. doi:https://doi.org/10.1523/JNEUROSCI.1428-09.2009.
Haenschel C, Bittner RA, Haertling F, Rotarska-Jagiela A, Maurer K, Singer W, et al. Contribution of impaired early-stage visual processing to working memory dysfunction in adolescents with schizophrenia. Arch Gen Psychiatry 2007;64:1229. https://doi.org/10.1001/archpsyc.64.11.1229.
Hanslmayr S, Staudigl T, Fellner M-C. Oscillatory power decreases and long-term memory: the information via desynchronization hypothesis. Front Hum Neurosci 2012;6:74. https://doi.org/10.3389/fnhum.2012.00074.
Harmony T. The functional significance of delta oscillations in cognitive processing. Front Integr Neurosci 2013;7:83. https://doi.org/10.3389/fnint.2013.00083.
Huynh H, Feldt LS. Estimation of the box correction for degrees of freedom from sample data in randomized block and split-plot designs. J Educ Stat 1976;1:69–82. https://doi.org/10.2307/1164736?ref=no-x-route:35a704d5df74c9df3b336a8bf049147b.
Hyvärinen A. Fast and robust fixed-point algorithms for independent component analysis. IEEE Trans Neural Networks 1999;10:626–34. https://doi.org/10.1109/72.761722.
Hyvärinen A, Oja E. Independent component analysis: algorithms and applications. Neural Networks 2000;13:411–30. https://doi.org/10.1016/S0893-6080(00)00026-5.
Ince NF, Pellizzer G, Tewfik AH, Nelson K, Leuthold A, McClannahan K, et al. Classification of schizophrenia with spectro-temporo-spatial MEG patterns in working memory. Clin Neurophysiol 2009;120:1123–34. https://doi.org/10.1016/j.clinph.2009.04.008.
Itthipuripat S, Wessel JR, Aron AR. Frontal theta is a signature of successful working memory manipulation. Exp Brain Res 2013;224:255–62. https://doi.org/10.1007/s00221-012-3305-3.
Jeong J, Williams WJ. A new formulation of generalized discrete-time time-frequency distributions. In: Proc. IEEE ICASSP-91; 1991. p. 3189–92.
Kang SS, Sponheim SR, Chafee MV, MacDonald AW. Disrupted functional connectivity for controlled visual processing as a basis for impaired spatial working memory in schizophrenia. Neuropsychologia 2011;49:2836–47. https://doi.org/10.1016/j.neuropsychologia.2011.06.009.
Khader PH, Rösler F. EEG power changes reflect distinct mechanisms during long-term memory retrieval. Psychophysiology 2011;48:362–9. https://doi.org/10.1111/j.1469-8986.2010.01063.x.
Kim J, Glahn DC, Nuechterlein KH, Cannon TD. Maintenance and manipulation of information in schizophrenia: further evidence for impairment in the central executive component of working memory. Schizophr Res 2004;68:173–87. https://doi.org/10.1016/S0920-9964(03)00150-6.
Koyama Y, Hattori T, Shimizu S, Taniguchi M, Yamada K, Takamura H, et al. DBZ (DISC1-binding zinc finger protein)-deficient mice display abnormalities in basket cells in the somatosensory cortices. J Chem Neuroanat 2013;53:1–10. https://doi.org/10.1016/j.jchemneu.2013.07.002.
Kriegeskorte N, Simmons WK, Bellgowan PSF, Baker CI. Circular analysis in systems neuroscience: the dangers of double dipping. Nat Neurosci 2009;12:535–40. https://doi.org/10.1167/8.6.88.
Leiderman EA, Strejilevich SA. Visuospatial deficits in schizophrenia: central executive and memory subsystems impairments. Schizophr Res 2004;68:217–23. https://doi.org/10.1016/S0920-9964(03)00215-9.
Lukoff D, Nuechterlein H, Ventura J. Manual for the expanded brief psychiatric rating scale. Schizophr Bull 1986;12:594.
Lynn PA, Kang SS, Sponheim SR. Impaired retrieval processes evident during visual working memory in schizophrenia. Schizophr Res Cogn 2016;5:47–55. https://doi.org/10.1016/j.scog.2016.07.002.
Lynn PA, Sponheim SR. Disturbed theta and gamma coupling as a potential mechanism for visuospatial working memory dysfunction in people with schizophrenia. Neuropsychiatr Electrophysiol 2016;2:7. https://doi.org/10.1186/s40810-016-0022-3.
McMenamin BW, Shackman AJ, Maxwell JS, Bachhuber DRW, Koppenhaver AM, Greischar LL, et al. Validation of ICA-based myogenic artifact correction for scalp and source-localized EEG. Neuroimage 2010;49:2416–32. https://doi.org/10.1016/j.neuroimage.2009.10.010.
Medendorp WP, Kramer GFI, Jensen O, Oostenveld R, Schoffelen JM, Fries P. Oscillatory activity in human parietal and occipital cortex shows hemispheric lateralization and memory effects in a delayed double-step saccade task. Cereb Cortex 2007;17:2364–74. https://doi.org/10.1093/cercor/bhl145.
Miyake A, Shah P. Models of working memory: mechanisms of active maintenance and executive control. New York, NY: Cambridge University Press; 1999. doi: https://doi.org/10.1017/CBO9781139174909.
Mohr HM. Content- and task-specific dissociations of frontal activity during maintenance and manipulation in visual working memory. J Neurosci 2006;26:4465–71. https://doi.org/10.1523/JNEUROSCI.5232-05.2006.
Palva S, Kulashekhar S, Hamalainen M, Palva JM. Localization of cortical phase and amplitude dynamics during visual working memory encoding and retention. J Neurosci 2011;31:5013–25. https://doi.org/10.1523/JNEUROSCI.5592-10.2011.
Palva S, Palva JM. New vistas for α-frequency band oscillations. Trends Neurosci 2007;30:150–8. https://doi.org/10.1016/j.tins.2007.02.001.
Phillips KG, Uhlhaas PJ. Neural oscillations as a translational tool in schizophrenia research: rationale, paradigms and challenges. J Psychopharmacol 2015;29:155–68. https://doi.org/10.1177/0269881114562093.
Piercy M, Hécaen H, De Ajuriaguerra J. Constructional apraxia associated with unilateral cerebral lesions-left and right sided cases compared. Brain 1960;83:225–42. https://doi.org/10.1093/brain/83.2.225.
Pittman-Polletta BR, Kocsis B, Vijayan S, Whittington MA, Kopell NJ. Brain rhythms connect impaired inhibition to altered cognition in schizophrenia. Biol Psychiatry 2015;77:1020–30. https://doi.org/10.1016/j.biopsych.2015.02.005.
Roopun AK. Temporal interactions between cortical rhythms. Front Neurosci 2008;2:145–54. https://doi.org/10.3389/neuro.01.034.2008.
Rotstein HG, Pervouchine DD, Acker CD, Gillies MJ, White JA, Buhl EH, et al. Slow and fast inhibition and an H-current interact to create a theta rhythm in a model of CA1 interneuron network. J Neurophysiol 2005;94:1509–18.
Roux F, Uhlhaas PJ. Working memory and neural oscillations: alpha-gamma versus theta-gamma codes for distinct WM information? Trends Cogn Sci 2014;18:16–25. https://doi.org/10.1016/j.tics.2013.10.010.
Sauseng P, Griesmayr B, Freunberger R, Klimesch W. Control mechanisms in working memory: a possible function of EEG theta oscillations. Neurosci Biobehav Rev 2010;34:1015–22. https://doi.org/10.1016/j.neubiorev.2009.12.006.
Schmiedt C, Brand A, Hildebrandt H, Basar-Eroglu C. Event-related theta oscillations during working memory tasks in patients with schizophrenia and healthy controls. Cogn Brain Res 2005;25:936–47. https://doi.org/10.1016/j.cogbrainres.2005.09.015.
Stephane M, Ince NF, Leuthold A, Pellizzer G, Tewfik AH, Surerus C, et al. Temporospatial characterization of brain oscillations (TSCBO) associated with subprocesses of verbal working memory in schizophrenia. Clin EEG Neurosci 2008;39:194–202. https://doi.org/10.1177/155005940803900409.
Uhlhaas PJ, Haenschel C, Nikolić D, Singer W. The role of oscillations and synchrony in cortical networks and their putative relevance for the pathophysiology of schizophrenia. Schizophr Bull 2008;34:927–43. https://doi.org/10.1093/schbul/sbn062.
Uhlhaas PJ, Singer W. Abnormal neural oscillations and synchrony in schizophrenia. Nat Rev Neurosci 2010;11:100–13. https://doi.org/10.1038/nrn2774.
Ventura V, Paciorek CJ, Risbey JS. Controlling the proportion of falsely rejected hypotheses when conducting multiple tests with climatological data. J Clim 2004;17:4343–56. https://doi.org/10.1175/3199.1.
Vijayan S, Kopell NJ. Thalamic model of awake alpha oscillations and implications for stimulus processing. Proc Natl Acad Sci USA 2012;109:18553–8. https://doi.org/10.1073/pnas.1215385109.
Wang X-J. Neurophysiological and computational principles of cortical rhythms in cognition. Physiol Rev 2010;90:1195–268. https://doi.org/10.1152/physrev.00035.2008.
Whittington M, Traub R, Kopell N, Ermentrout B, Buhl E. Inhibition-based rhythms: experimental and mathematical observations on network dynamics. Int J Psychophysiol 2000;38:315–36. https://doi.org/10.1016/S0167-8760(00)00173-2.
Yuval-Greenberg S, Tomer O, Keren AS, Nelken I, Deouell LY. Transient induced gamma-band response in EEG as a manifestation of miniature saccades. Neuron 2008;58:429–41. https://doi.org/10.1016/j.neuron.2008.03.027.